Assembly Properties of Dominant and Recessive Mutations in the Small Mouse Neurofilament (NF-L) Subunit

Steven R. Gill, Philip C. Wong, Mervyn J. Monteiro, and Don W. Cleveland

Department of Biological Chemistry, The Johns Hopkins University School of Medicine, Baltimore, Maryland 21205

Abstract. We have generated a set of amino- and carboxy-terminal deletions of the NF-L neurofilament gene and determined the assembly properties of the encoded subunits after coexpression with vimentin or wild-type NF-L. NF-L molecules missing >30% (31 amino acids of the head) or 90% (128 amino acids of the tail) failed to incorporate into intermediate filament networks. Carboxy-terminal deletions into the rod domain yield dominant mutants that disrupt arrays assembled from wild-type subunits, even when present at levels of ≈2% of the wild-type subunits. Even mutants retaining 55% of the tail (61 amino acids) disrupt normal arrays when accumulated above ≈10% of wild-type subunits. Since deletion of >90% of the head domain produces "recessive" assembly incompetent subunits that do not affect wild-type filament arrays, whereas smaller deletions yield efficient network disruption, we conclude that some sequence(s) in the head domain (within residues 31–87) are required for the earliest steps in filament assembly. Insertional mutagenesis in the nonhelical spacer region within the rod domain reveals that as many as eight additional amino acids can be tolerated without disrupting assembly competence.

Most higher eukaryotic cells contain cytoplasmic arrays of 8–10-nm filaments known collectively as intermediate filaments (IFs).[1] Although the underlying subunits are encoded by at least five distinct gene families (vimentin in mesenchymal cells, keratins in epithelial cells, desmin in muscle cells, glial fibrillary acidic protein in glial cells, and neurofilaments [NFs] in neurons; see Geisler and Weber, 1982; Steinert and Roop, 1988), the subunits are all characterized by a conserved central α helical coiled-coil domain of ~310 amino acids (Geisler and Weber, 1986; Franke, 1987). The presence of similar structural motifs has led to discovery of the nuclear lamin subunits to be members of the IF family (McKeon et al., 1986; Fisher et al., 1986) and to identification of three additional IF proteins expressed in different subsets of neurons (peripherin, a vimentin-like IF expressed in a subset of peripheral neurons [Portier et al., 1984; Parysek and Goldman, 1987; Leonard et al., 1988], α-internexin, an NF-like polypeptide [Fliegner et al., 1990] and nestin, an IF subunit expressed in neuroepithelial stem cells [Lendahl et al., 1990]). The amino-terminal head and carboxy-terminal tail regions that flank this structurally conserved helical domain vary among the subunits both in sequence and length. This is particularly true for the carboxy-terminal tails of mammalian NFs, which unlike most IFs, are coassembled from three subunits: NF-L, NF-M, and NF-H. The three polypeptides (whose actual sizes are ~65 [Lewis and Cowan, 1986], 95–102 [Levy et al., 1987; Napolitano et al., 1987; Myers et al., 1987], and 110–115 kD [Julien et al., 1987; Lees et al., 1988]) all contain the 310 amino acid helical domain but differ in size primarily by their carboxy-terminal tail segments (Geisler et al., 1983). Although the arrangement of the subunits in the final polymer is not established (reviewed in the companion paper, Wong and Cleveland, 1990), each NF component is almost certainly an integral IF subunit (e.g., Geisler and Weber, 1981; Liem and Hutchinson, 1982; Totutake et al., 1984; Hisanaga and Hirokawa, 1990).

Despite plausible arguments for the function of some IFs in the maintenance of various cell structures, there is as yet no experimental demonstration of such putative function(s). Certainly in cultured cells the known cytoplasmic IFs can be completely dispensable (Gawlitta et al., 1981; Klymkowsky, 1981; Lin and Feramisco, 1981; Venetianer et al., 1983; Herdberg and Chen, 1986). On the other hand, in mature myelinated axons NFs are the most abundant cytoskeletal component, outnumbering microtubules by an order of magnitude (Friede and Samorajski, 1970). NFs are incorporated into axons primarily after nerve targeting (Berthold, 1978) and NF accumulation correlates tightly with radial growth of the axon both in normal development (e.g., during myelination; Muma, N., and P. Hoffman, unpublished data) and during axonal regeneration after axonal injury (Hoffman et al., 1987). Since NF number per cross-sectional area re-

M. J. Monteiro's present address is Department of Neurology and the Medical Biotechnology Center, University of Maryland School of Medicine, Baltimore, MD 21201.

1. *Abbreviations used in this paper*: IF, intermediate filament; MSV, murine sarcoma virus; NF, neurofilament.

mains nearly constant during these events, we and our colleagues have proposed that NFs are intrinsic determinants of axonal diameter (Hoffman et al., 1984, 1985, 1987; Hoffman and Cleveland, 1988).

To determine how the head, rod, and tail domains influence NF assembly and to identify altered NF-L subunits that could be used to disrupt the assembly of wild-type NF-L in transgenic animals, we have now used DNA transfection to force expression of specifically altered NF-L subunits in cultured cells that express either wild-type vimentin and/or NF-L. By using indirect immunofluorescence to follow the assembly properties of the mutant and endogenous IF subunits, we identify a series of dominant assembly disrupting mutations that serve as substoichiometric poisons of normal filament organization. We also determine that competence of NF-L to assemble into IF arrays requires not only the rod domain, but also substantial portions of the head and tail segments.

Materials and Methods

Construction of Carboxy-Terminal Deletions of NF-L

To prepare a series of NF-L genes deleted in their carboxy-terminal sequences, we first constructed pMSV-NF-LcDNA. To do this, we replaced the Bgl II–Eco RI fragment of pMSV-NF-L (which contains the mouse NF-L gene linked to the murine sarcoma virus (MSV) long terminal repeat (LTR) promoter; Monteiro and Cleveland, 1989) with the Bgl II–Eco RI fragment from a previously described NF-L cDNA (Lewis and Cowan, 1985). This yielded a complete, intronless mouse NF-L sequence linked to the MSV-LTR. To generate a set of NF-L carboxy-terminal deletions, the pMSV-NF-LcDNA was digested with Eco RI, deleted with exonuclease III, and blunted with mung bean nuclease. The deleted DNA was then digested with Bam HI, which cleaves at a unique site in the pUC19 polylinker at the 3′ end of the NF-L cDNA. The resulting blunt-ended/Bam HI fragments were gel purified. A common carboxy-terminal tag comprised of a 12 amino acid epitope from the human c-*myc* protein (Munro and Pelham, 1987) was then added to each deletion. This was achieved by synthesizing a "myc-tag" cassette and ligating it just 5′ to the complete 3′ untranslated and ~1.5 kb of 3′ flanking sequences of the NF-L genomic clone (creating pMYC-0 [Fig. 2 *B*]). To insert this cassette into the deleted NF-L cDNA, pMYC-0 was linearized with Sal I or Nco I, blunted with Klenow fragment and cleaved with Bam HI. The resulting "myc-tag" was gel purified and ligated to the set of pMSV-NF-LcDNA deletions to produce the carboxy-terminal deletions series, pNFL-CΔ*x*, where *x* denotes the number of amino acids removed from the carboxy terminus of NF-L cDNA (Figs. 1 and 2).

Construction of Amino-Terminal Deletions of NF-L

The amino-terminal deletions of NF-L were generated using pNFL-CΔ11 as the starting construct (see Fig. 1). The protein encoded by this gene is deleted by 11 amino acids at the carboxy-terminal end where the myc-tag cassette has been inserted. Amino-terminal deletions were generated by first linearizing pNFL-CΔ11 at the Cla I site (that lies within the MSV-LTR), followed by treatment with exonuclease III and mung bean nuclease. The deleted DNAs were digested at the unique Bam HI site located at the 3′ end of the myc-tag and the blunted-Bam HI fragments were gel purified. A cassette, pNF5-ATG (see Wong and Cleveland, 1990) was used to restore the promoter, 5′ untranslated region, and ATG initiation codon of each deleted construct. pNF5-ATG was linearized with Sal I, blunted with mung bean nuclease, and digested at the unique Bam HI site. The pNF5-ATG fragments were gel purified and ligated to the appropriate blunted-Bam HI NF-L amino-terminal deletion fragments. This produced pNFL-NΔ*y*, where *y* represents the number of amino acids deleted from the amino terminus (displayed schematically in Fig. 7).

Construction of Internal Amino-Terminal Deletions of NF-L

Internal deletions within the amino-terminal head domain of NF-L were constructed using the previously described pMSV-NF-L genomic clone (see Monteiro and Cleveland, 1989). The gene was linearized at the Sma I site (at codon 23) and treated with Bal 31 nuclease to generate internal deletions. The DNA was subsequently blunted with S1 nuclease and self-ligated. This yielded the constructs pMSV-NFLΔ*x*-*y*, where *x* and *y* denote the amino acid end points of the deletions.

Insertion of Amino Acids between Coils 1b and 2 of pMSV-NF-LcDNA

To generate a set of amino acid additions within the 22 amino acid domain between coils 1b and 2 of NF-L, single or multiple copies of Bam HI linkers (New England Biolabs, Beverly, MA) were inserted into a unique Bgl II site that lies between codons 242 and 243 (eight amino acids into the linker region) of pNFL-CΔ11 (Fig. 9). Phosphorylated 12-mer Bam HI linkers were first self-ligated to completion. The ligated linkers were subsequently partially digested with Bam HI to generate a set of linker cassettes of 12, 24, 36, etc., base pairs. pNFL-CΔ11 was linearized with Bgl II and gel purified. The linker cassettes were ligated into the Bgl II site of pNFL-CΔ11, generating a set of genes, pNFL+*z*, where *z* denotes the number of amino acids inserted between coils 1b and 2 (see schematic in Fig. 9). A five amino acid insertion was constructed by a similar method, except that the sequence inserted was a 15-base segment of the polylinker from plasmid BluescriptKS+.

DNA Sequencing

Plasmid DNAs from the pNFL-CΔ*x*, pNFL-NΔ*y*, pNFL-NΔ*x*-*y*, and pNFL+*z* series were partially sequenced by the dideoxy-chain termination method to determine the deletion and insertion end points.

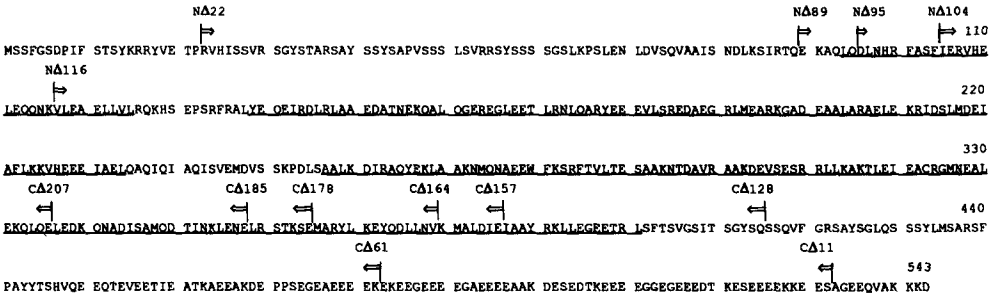

Figure 1. Positions of amino- and carboxy-terminal truncation mutants in the primary sequence of the mouse NF-L polypeptide. The one letter code has been used to display the primary sequence of the mouse NF-L polypeptide, as deduced from DNA sequencing (Lewis and Cowan, 1986). Residues within the predicted helical rod domain (Geisler et al., 1985) are underlined. Positions where amino-terminal and carboxy-terminal mutants of NF-L begin or end are marked.

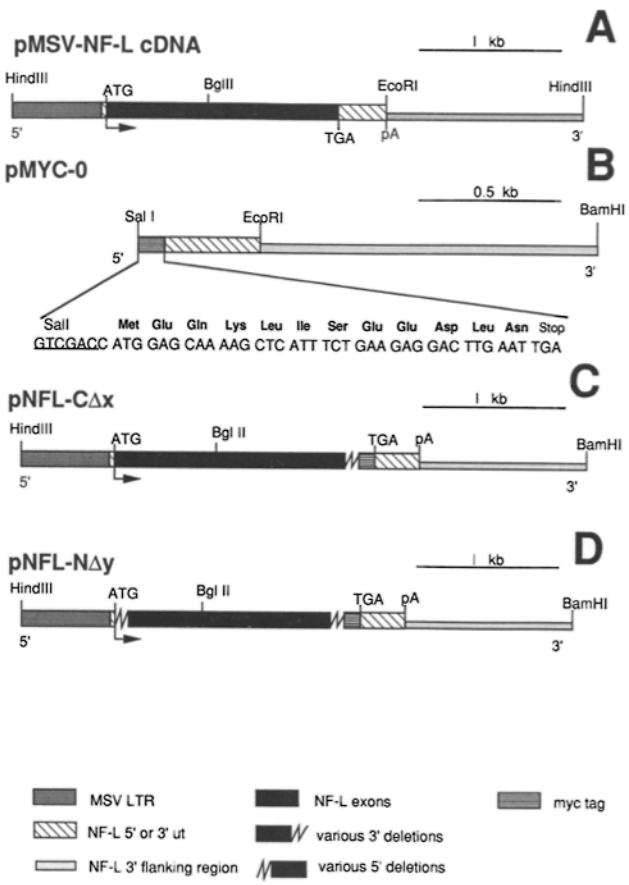

Figure 2. Gene constructs for expression of carboxy-terminal truncations of NF-L. (*A*) Schematic drawing of the MSV-NF-LcDNA gene. (*B*) Schematic of pMYC-0, which carries the sequences encoding the 12 amino acid c-myc tag (Evan et al., 1985) followed by a TGA stop codon and the 3′ untranslated and 3′ flanking regions of the mouse NF-L gene. (*C*) Schematic of the pNFL-CΔx series of genes deleted to varying extents into the carboxy-terminal coding sequence of NF-L. (*D*) Schematic of the pNFL-NΔy series of genes deleted to varying extents in the amino-terminal coding sequence of NF-L.

Tissue Culture and Transfection

Mouse fibroblast L cells and an L cell line (MSV-NF9) that stably expresses NF-L (Monteiro and Cleveland, 1989) were maintained in DME medium supplemented with 10% fetal bovine serum. Cells were transiently transfected using the DEAE-dextran method (Lopata et al., 1984). Cells were typically analyzed 40 h posttransfection.

SDS Gel Electrophoresis and Immunoblotting

For detection of total cellular protein, cells were washed twice with PBS, lysed with 300 μl of 50 mM Tris-HCl (pH 6.8), 0.5% SDS, boiled for 5 min, and briefly centrifuged to remove genomic DNA. Protein concentrations were determined with the bicinchoninic acid assay (Smith et al., 1985). Before electrophoresis on 10% SDS polyacrylamide gels (Laemmli, 1970), equal amounts of protein (in Laemmli gel sample buffer containing 2% β-mercaptoethanol) were boiled for 5 min. After electrophoresis, the separated proteins were electroblotted to nitrocellulose membranes (type BA83; Schleicher & Schuell, Inc., Keene, NH) and incubated with primary and secondary antibodies as previously described (Lopata and Cleveland, 1987).

To prepare soluble and insoluble fractions, cells were washed twice with PBS. Soluble proteins were extracted by incubating the cells in stabilizing buffer (4 M glycerol, 100 mM Pipes, pH 6.9 and 1 mM EGTA) containing 0.5% Triton X-100. Soluble proteins were removed and the remaining insoluble proteins were dissolved in 300 μl of 50 mM Tris-HCl, pH 6.8, 0.5% SDS. Protein concentration was again determined using the bicinchoninic acid assay and equal amounts of protein were prepared for electrophoresis as indicated above. For detection of NF-L protein tagged with the myc epitope, the blotted membranes were first incubated with a mouse monoclonal antibody against myc (Mycl-9E10; Evan et al., 1985) followed by ^{125}I-labeled sheep anti-mouse antibody (Amersham Corp., Arlington Heights, IL).

For quantitation of myc-tagged molecules, the myc epitope was expressed as a bacterial fusion protein with an amino-terminal 32-kD segment of the bacterial trpE protein (as described in the companion paper [Wong and Cleveland, 1990]). By comparing the intensity of staining of known amounts of an induced bacterial extract with a twofold dilution series of known amounts of bovine albumin (from a solution whose concentration was determined by absorbance [A_{260} (1 mg/ml) = 0.67]), the concentration of the trpE-myc fusion (in micrograms per milliliter) in the extract was calculated. In every experiment, to provide a series of internal standards representing known amounts of the myc epitope, a dilution series of such a bacterial extract containing known amounts of this fusion protein were immunoblotted in parallel with cell extracts from transfected cells. By densitometric scanning of the signals on the resultant autoradiographs, a standard curve was constructed and the amount of myc tagged protein (in micrograms) present in each experimental sample was determined, after correcting for the differences in molecular mass between the trpE-myc fusion and the NF-L/myc tagged polypeptides.

By using dilutions of partially purified vimentin, an analogous method has previously been used to determine that vimentin comprises 1–2% of cell protein in mouse L cells (Monteiro and Cleveland, 1989).

Immunofluorescence Staining

Transfected cells grown on coverslips were washed for 30 s at room temperature in stabilization buffer, extracted for 30 s in stabilization buffer containing 0.5% Triton X-100 at room temperature, and again washed for 30 s in stabilization buffer. The coverslips were then plunged into −20°C methanol for 5 min and then rehydrated in PBS for at least 10 min. Both primary and secondary antibodies were diluted in PBS containing 1% BSA and incubated on the coverslips for 30 min at room temperature. The coverslips were washed in PBS to remove unbound antibodies and mounted on glass slides using Aqua-mount (Lerner Laboratories, New Haven, CT). An Olympus BH-2 microscope was used to examine the stained cells using epifluorescence optics and photographs were taken on Kodak TMAX film. Primary antibodies used were a partially concentrated culture supernatant from monoclonal antibody Mycl-9E10 (Evan et al., 1985), a monoclonal antibody against NF-L (used at 1:2; Boehringer Mannheim Diagnostics, Inc., Indianapolis, IN), a goat polyclonal antibody to vimentin (used at 1:50; ICN Immunobiologicals, Costa Mesa, CA), and a rabbit polyclonal antibody to NF-L (used at 1:500; the kind gift of Dr. G. Shaw [University of Florida, Gainesville, FL]). Affinity-purified fluorescein-conjugated (for Mycl-9E10 and the NF-L monoclonal) and rhodamine-conjugated (for vimentin and the NF-L polyclonal) secondary antibodies (obtained from ICN Immunobiologicals) were used at 1:40 dilutions.

Results

Assembly Properties of Carboxy-Terminal Truncations of NF-L

NF-L is thought to consist of three domains: a 93 amino acid head, a 308 amino acid helical region (using the borders proposed by Geisler et al. [1985]), and a 142 amino acid tail segment. To test the influence of the tail sequences on NF-L assembly properties, we used exonuclease III to generate a series of carboxy-terminal mutations starting with pMSV-NF-LcDNA, a chimeric gene comprised of the strong transcriptional promoter from MSV, a cDNA sequence containing the complete protein coding region of mouse NF-L (including most of the 5′ and 3′ untranslated regions) and ~1.5 kb of the 3′ flanking region of the authentic NF-L gene (Fig. 2 *A*). To facilitate detection of the product encoded by each mutant gene, we tagged the carboxy terminus of each mutant polypeptide with a 12 amino acid segment (from the human

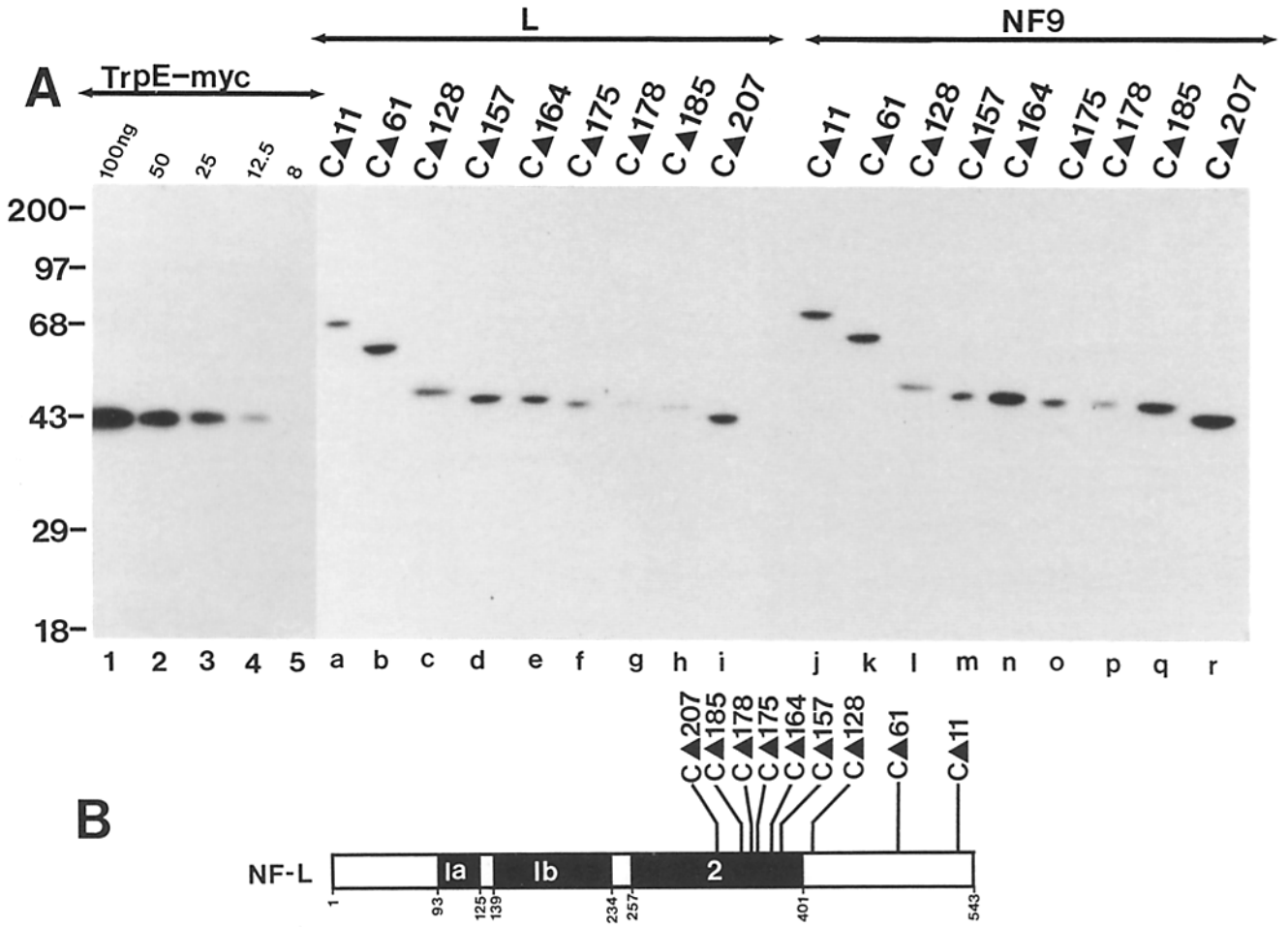

Figure 3. Immunoblot detection of NF-L polypeptides deleted in carboxy-terminal tail sequences, after transient transfection of pNFL-CΔ*x* constructs into either mouse L cells or MSV-NF9 cells. (*A*) Immunoblot detection of NF-L polypeptides accumulated 40 h after transfection. Extracts of total cellular proteins (50 μg per extract) from cells transfected with each mutant were analyzed by immunoblotting. Mutant NF-L polypeptides were detected using an anti-myc-tag monoclonal antibody. Lanes *a–i*, protein extracts from L cells transfected with the corresponding pNFL-CΔ*x* DNAs as indicated; lanes *j–r*, protein extracts from MSV-NF9 cells transfected with the respective pNFL-CΔ*x* DNAs. Molecular mass markers (in kilodaltons) are indicated at the left. Lanes *1–5* display immunoblots of a dilution series of a bacterial extract containing known amounts of a hybrid protein comprised of trpE linked to the myc tag. The corresponding amounts (in nanograms) of trpE-myc fusion are noted at the top of each lane. (*B*) Schematic drawing of the NFL-cΔ*x* polypeptides. The helical domain is represented by the closed rectangles and the deletion endpoints of specific mutants are indicated.

c-*myc* protein—Fig. 2, *B* and *C*). The deletion end point of each mutant was determined by DNA sequencing and constructs in which the NF-L and c-*myc* tag sequences were linked in frame were identified. Each mutant construct (Fig. 2 *C*) is denoted by pNFL-CΔ*x*, where *x* refers to the number of amino acids removed from the carboxy terminus of NF-L (precise end points within the NF-L sequence are shown in Fig. 1).

To confirm that the expected protein product did accumulate after transient transfection of each mutant gene, extracts of total cellular proteins were analyzed 40-h posttransfection of mouse L cells. Products of the transfected genes were identified using immunoblotting with a monoclonal antibody that recognizes the c-*myc* tag sequence (but not the corresponding domain of the endogenous mouse c-*myc* polypeptide). As shown in Fig. 3 *A*, a polypeptide of the expected size was accumulated for each mutant (beginning with the smallest deletion of 11 amino acids through the largest deletion of 207 amino acids). By parallel immunoblotting of known amounts of a bacterial fusion protein comprised of the bacterial trpE protein linked to the c-myc tag (Fig. 3 *A*, lanes *1–5*) and by using indirect immunofluorescence to determine that 20% of the cells were successfully transfected, we calculated that the mutant NF-L subunits accumulated to between ~0.05 and 0.2% of total cell protein. Since vimentin, the endogenous IF in these cells, comprises ~1–2% of cell protein (Monteiro and Cleveland, 1989), the average molar proportions of NF-L to vimentin ranged between 1:10 and 1:40.

The ability of each mutant to coassemble with vimentin was determined 40 h following transient transfection using double immunofluorescence with the myc antibody to localize each NF-L mutant and a polyclonal antibody to vimentin to report the endogenous IF array. Substitution of the carboxy-terminal 11 amino acids of NF-L with the c-*myc* tag (NFL-CΔ11) yielded an NF-L subunit that coassembled into the endogenous vimentin network in L cells (Fig. 4, *A* and

B). Immunoblot analysis of soluble proteins and of those remaining in the insoluble cytoskeletal fraction confirmed that essentially all myc tagged NF-L was found in the cytoskeletal fraction (Fig. 5, lanes *a* and *b*). Since coassembly of NFL-CΔ11 was seen in all cells expressing this construct, we interpret this to mean that neither the presence of the tag nor the loss of the carboxy-terminal sequences affected the competence of the NF-L subunit to coassemble with vimentin.

A different finding emerged following transfection of an NF-L gene deletion in which 44% of the tail (the carboxy-terminal 61 amino acids) were deleted. The shortened NF-L subunit was found colocalized with the vimentin IF array (Fig. 4, *C* and *D*), but only in 30% of the cells. Although this clearly demonstrated the retention of competence of this subunit for coassembly, in two-thirds of the transfected cells expression of pNFL-CΔ61 yielded a very different phenotype (Fig. 4, *E* and *F*). In these cases, the truncated NF-L subunits were not fully assembled. In half of these, the mutant NF-L was localized to punctate aggregates that were distributed throughout the cytoplasm, with the highest concentration found in the perinuclear region. There was no evidence of filamentous NF-L in these cells and in fact the vimentin array was partially disrupted (Fig. 4 *F*). (The cell shown is probably binucleate, but since the parental L cell line has a high proportion of binucleates [~25%], we do not suggest that this mutant affects nuclear structure, etc.) Immunoblot analysis of soluble and cytoskeletal fractions confirmed that all of the truncated NF-L remained in the insoluble fraction (Fig. 5, lanes *c* and *d*).

Further carboxy-terminal deletion to remove 91% of the tail domain (NFL-CΔ128) invariably yielded a failure of the NF-L subunit to assemble normally (Fig. 4 *G*). This was accompanied by a partial fragmentation or disruption of vimentin arrays, particularly in the peripheral areas of the cytoplasm where few, if any, filaments remained (Fig. 4 *H*). In fact, in 50% of the cells expressing NFL-CΔ128 (presumably those that express the highest amount of truncated NF-L), none of the vimentin was accumulated into obvious filaments (not shown). A further curious finding was that in many cells not all of the cytoplasmic aggregates containing NF-L stained positive for vimentin (compare Fig. 4, *G* and *H*). Deletion of 15 or 22 amino acids into the predicted helical domain (NFL-CΔ157 and NFL-CΔ164, respectively) yielded assembly incompetent NF-L subunits in all transfected cells (Fig. 4, *I* and *K*): in most (90%), the vimentin array was also completely disrupted, although in a few (10%) some vimentin-containing filaments remained (Fig. 4 *J*). Particularly striking was that in 50% of NFL-CΔ164 expressing cells, in addition to punctate staining throughout the cytoplasm, most NF-L was accumulated into large spherical masses adjacent to or within the nucleus (Fig. 4 *M*). These nuclear-associated aggregates contained very little vimentin (Fig. 4 *N*), which remained restricted to the cytoplasm. Confocal microscopy confirmed that at least some of these aggregates were intranuclear (not shown), a pattern reminiscent of intranuclear particles of lamins accumulated in cells transfected with specific carboxy-terminal lamin mutants (Holtz et al., 1989). Indeed, like the example in Fig. 4 *M*, in almost all such cells the normal round appearance of the nucleus was deformed. However, double immunofluorescence experiments revealed no obvious disruption of lamin assembly, although a minor amount of colocalization of mutant and lamin could be observed (not shown). Why this truncated NF-L accumulates intranuclearly in a substantial fraction of NFL-CΔ164 expressing cells is uncertain, as is why it remains cytoplasmic in the remaining cells. An appealing possibility is the involvement of a cell cycle–dependent event, but this has not yet been experimentally verified.

All additional deletions into the rod domain (i.e., NFL-CΔ176 through NFL-CΔ207) yielded a uniform phenotype: all of these subunits were dominant, disruptors of the wild-type IF network (not shown) and continued to be found exclusively in the insoluble cytoskeletal fraction (Fig. 5, lanes *k–r*).

We conclude from these carboxy-terminal deletions that truncation into the rod domain yields an assembly incompetent NF-L subunit that when present in sufficient molar amounts is a dominant disruptor of wild-type vimentin arrays. Further, even an intact rod domain is insufficient for retention of assembly so that even when as much as 56% of the tail remains (NFL-CΔ61), some disruption of the normal array is observed (Fig. 4 *E*).

Carboxy-Terminal Mutations into the Rod Domain Disrupt Assembly of Wild-type NF-L

Although NF-L and vimentin are thought to coassemble together during the early phases of neurite development (e.g., Bignami et al., 1982), it was plausible that different interactions were required for efficient assembly with itself and for coassembly with vimentin. To test this, we expressed our series of carboxy-terminal NF-L mutants in cell line MSV-NF9, a mouse L cell derivative that stably expresses wild-type NF-L as the most abundant cell protein (at about four to eight times the level of endogenous vimentin; Monteiro and Cleveland, 1989). Again using double immunofluorescence to localize wild-type and mutant NF-L simultaneously, we found that deletion of the carboxy-terminal 11 residues of the tail yielded coassembly of mutant with wild-type (Fig. 6, *A–D*), just as was seen earlier when this mutant was coassembled with vimentin. Similarly, deletion of the final 61 amino acids yielded coassembly in some cells, although in most the mutant failed to assemble and partially disrupted the array of wild-type NF-L (Fig. 6, *C* and *D*). Deletion of additional tail sequences invariably yielded assembly incompetent subunits that disrupted the network assembled from the wild-type NF-L (e.g., mutant NFL-CΔ164; Fig. 6, *E* and *F*). These results completely paralleled those found earlier for coassembly with vimentin. We conclude that efficient coassembly of authentic and mutant NF-L requires ~80 amino acids of the tail domain, in addition to an intact rod segment.

Identification of Amino-Terminal Head Sequences Necessary for Assembly of NF-L

To test the effect of the 93 residue amino-terminal head domain on NF-L assembly, we constructed a series of amino-terminal deletions, beginning with a nearly wild-type NF gene (pNFL-CΔ11) carrying the myc tag at its carboxy terminus. Each amino-terminal mutant (the genes are shown schematically in Fig. 1 *D* and the polypeptides shown in Fig. 7 *A*) was transiently transfected into mouse L cells and assembly properties of the encoded subunits were analyzed by indirect immunofluorescence. Deletion of the first 22 amino

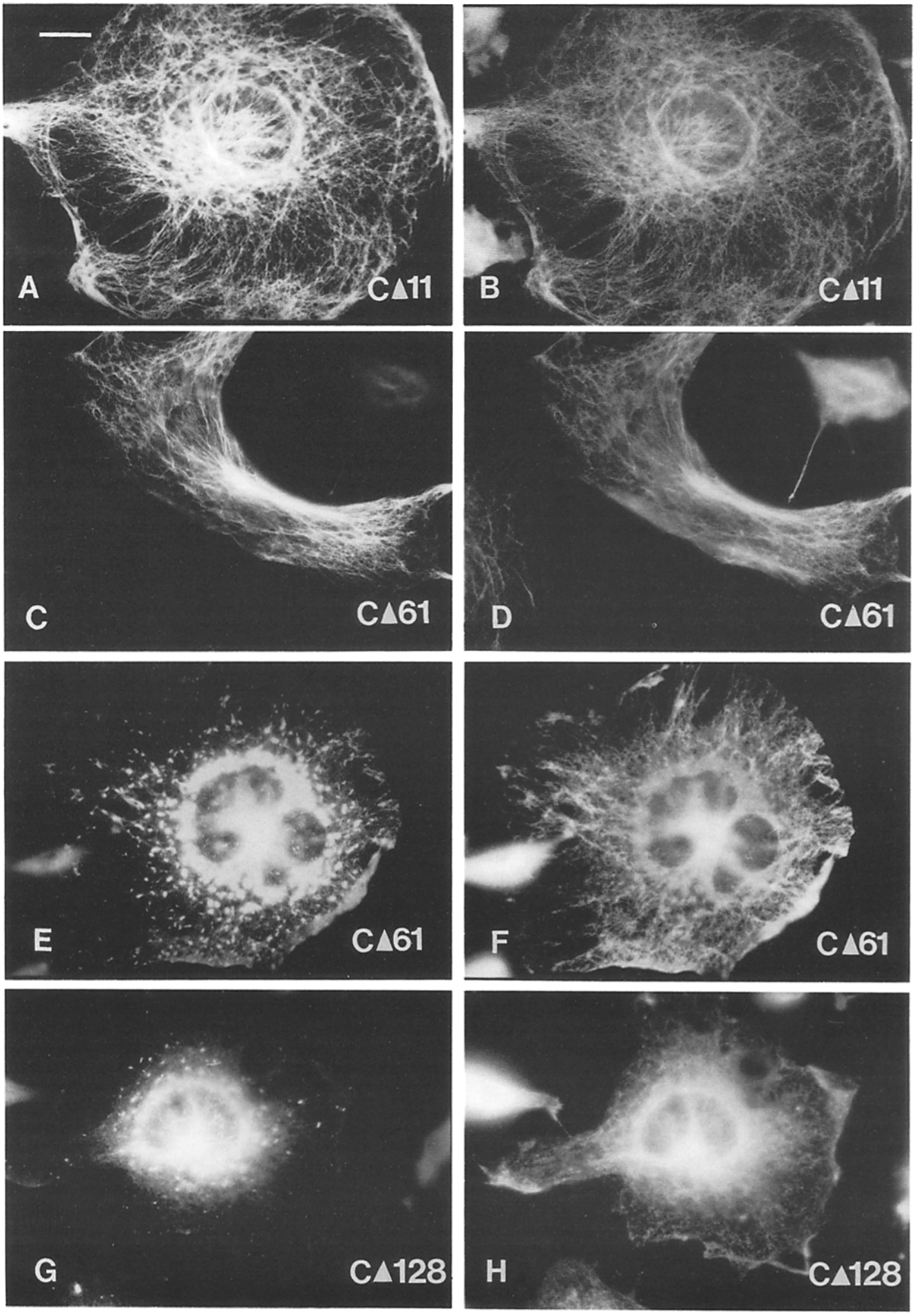
A
CΔ11
B
CΔ11
C
CΔ61
D
CΔ61
E
CΔ61
F
CΔ61
G
CΔ128
H
CΔ128

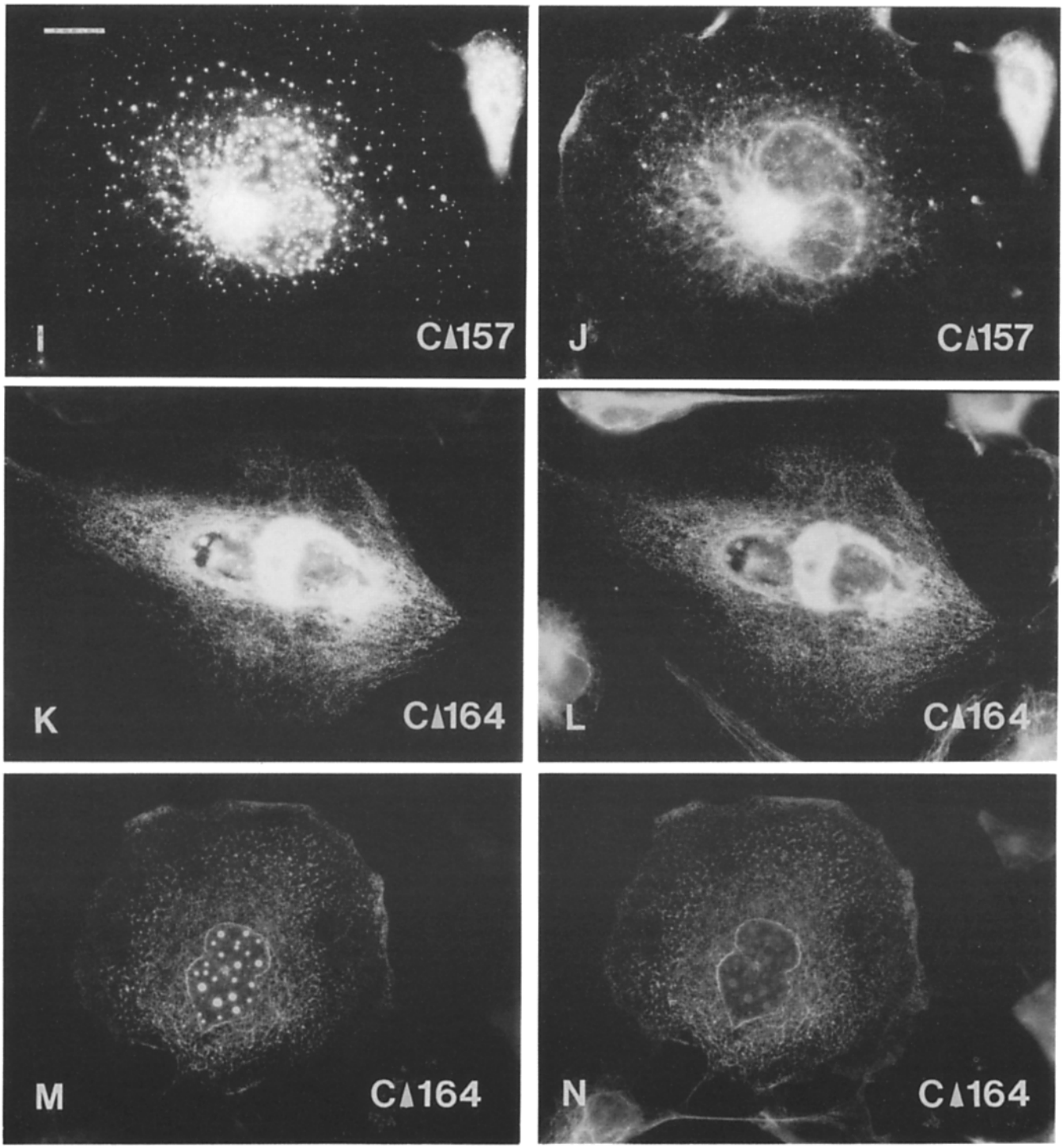

Figure 4. NF-L molecules missing >45% of the nonhelical carboxy-tail domain disrupt assembly of the vimentin array. Mouse L cells grown on coverslips were transfected with plasmids (*A* and *B*) pNFL-CΔ11, (*C–F*) pNFL-CΔ61, (*G* and *H*) pNFL-CΔ128, (*I* and *J*) pNFL-CΔ157, or (*K–N*) pNFL-CΔ164. (*A*, *C*, *E*, *G*, *I*, *K*, and *M*) The mutant NF-L polypeptides were visualized 40 h after transfection using the Mycl-9E10 monoclonal antibody (that recognizes the carboxy-terminal myc tag) followed by fluorescein-conjugated rabbit anti–mouse IgG; (*B*, *D*, *F*, *H*, *J*, *L*, and *N*) vimentin was visualized in the same transfected cells using double immunofluorescence with a goat polyclonal vimentin antibody followed by a rhodamine-conjugated rabbit anti–goat IgG. Bar, 10 μm.

acids yielded an NF-L subunit that was coassembled with the endogenous vimentin array in all transfected cells (Fig. 8, *A* and *B*). However, internal deletion of amino acids 18–31 of the amino terminus of an otherwise authentic (untagged) NF-L resulted in a very different phenotype: the mutant NF-L accumulated into aggregates that clustered around the nucleus, with a few scattered throughout the cytoplasm (Fig. 8 *C*). Although incompetent for coassembly into normal IF

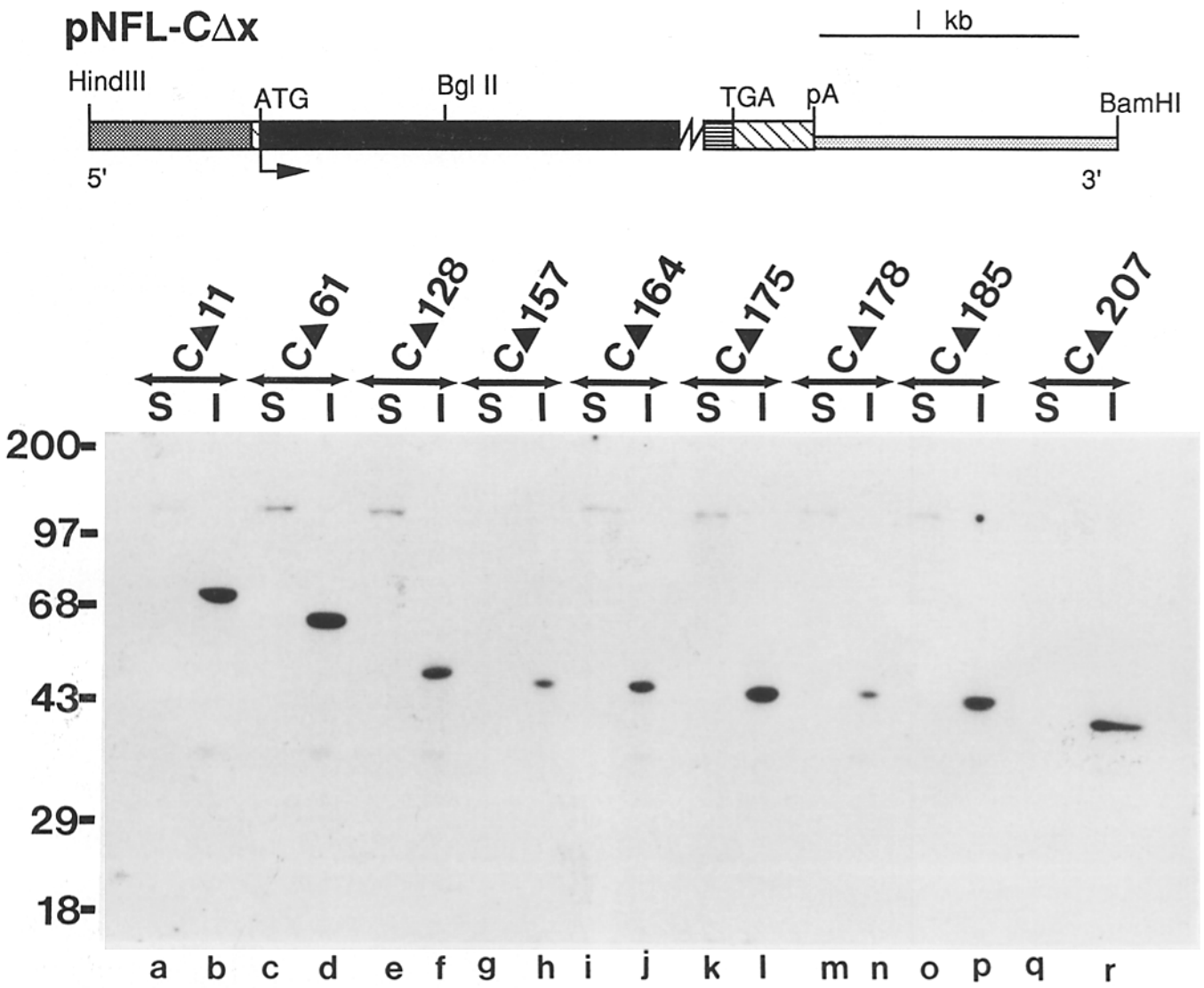

Figure 5. Accumulation of carboxy-truncated NF-L polypeptides into the insoluble cytoskeletal fraction. Soluble and insoluble cytoskeletal extracts were prepared from cells 40-h posttransfection with genes encoding tagged NF-L subunits truncated at their carboxy-termini. Equivalent proportions of soluble (*S*) and insoluble (*I*) fractions were immunoblotted using the myc tag monoclonal antibody to quantify the accumulation of NFL-CΔ*x* polypeptides. Extracts from mouse L cells transfected with (lanes *a* and *b*) pNFL-CΔ11, (lanes *c* and *d*) pNFL-CΔ61, (lanes *e* and *f*) pNFL-CΔ128, (lanes *g* and *h*) pNFL-CΔ157, (lanes *i* and *j*) pNFL-CΔ164, (lanes *k* and *l*) pNFL-CΔ175, (lanes *m* and *n*) pNFL-CΔ178, (lanes *o* and *p*) pNFL-CΔ185, and (lanes *q* and *r*) pNFL-CΔ207. Molecular mass markers in kilodaltons are indicated at the left.

networks, this mutant still efficiently associated with vimentin, causing its assembly to be largely disrupted (Fig. 8 *D*). Transfection of deletions that removed all but six amino acids or the entirety of the head (NFL-NΔ89 and NFL-NΔ95, respectively) produced a third phenotype. In all cells examined, the headless NF-L subunits accumulated into nonfilamentous cytoplasmic aggregates (Fig. 7, *E* and *G*). These aggregates contained little, if any, vimentin (Fig. 7, *F* and *H*), which remained assembled, albeit not in a completely wild-type array. Quantitative immunoblotting (Fig. 7 *B*) demonstrated that these headless constructs accumulated to between 0.02 and 0.5% of cell protein, levels similar to the carboxy-terminal assembly disruptors. Essentially identical results were observed when these mutants were coexpressed with wild-type NF-L in MSV-NF9 cells (data not shown).

We conclude that most of the head domain (including some or all of amino acids 31–89) of NF-L is required not only for assembly competence but also for efficient association with wild-type IF subunits.

Flexibility in the Linker Domain Within the Helical Rod of NF-L

The 308 amino acid domain of NF-L predicted to be helical contains two short segments of sequences that interrupt the hydrophobic heptad repeat. As shown schematically in Figs. 1 and 9, these domains (including helix breaking proline

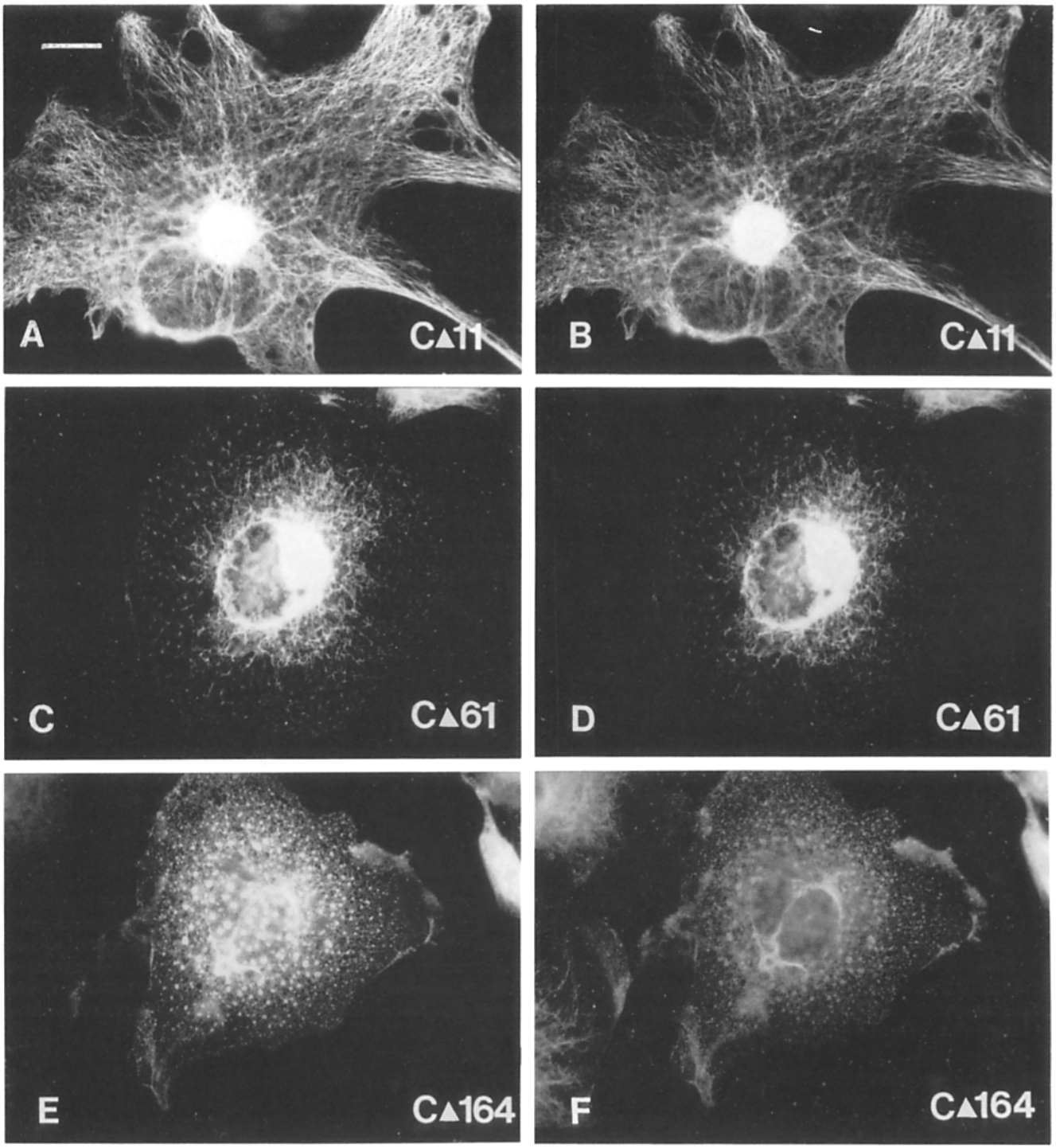

Figure 6. Expression of carboxy-terminal truncated NF-L polypeptides in L cells that stably express high levels of NF-L. MSV-NF9 cells grown on coverslips were transiently transfected with (*A* and *B*) pNFL-CΔ11, (*C* and *D*) pNFL-CΔ61 or (*E* and *F*) pNFL-CΔ164. Cells were stained 40 h after transfection with the Mycl-9E10 monoclonal antibody followed by fluorescein-conjugated rabbit anti-mouse IgG to visualize the NF-L mutant polypeptides and a rabbit polyclonal NF-L antibody followed by rhodamine-conjugated goat anti-rabbit IgG to detect the endogenous NF-L array. (*A*, *C*, and *E*) Mutant NF-L staining; (*B*, *D*, and *F*) wild-type NF-L staining. Bar, 10 μm.

residues) divide the predicted helix into three domains: coils 1a, 1b, and 2. Having documented that the rod domain was required, but not sufficient, for NF-L assembly, we next tested whether significant flexibility could be tolerated within the 21 amino acid linker domain that separates helices 1b and 2. To do this, we used linker mutagenesis of the tagged gene pNFL-CΔ11 to make 4, 5, 8, or 12 amino acid insertions within this putative hinge region. Each of these was

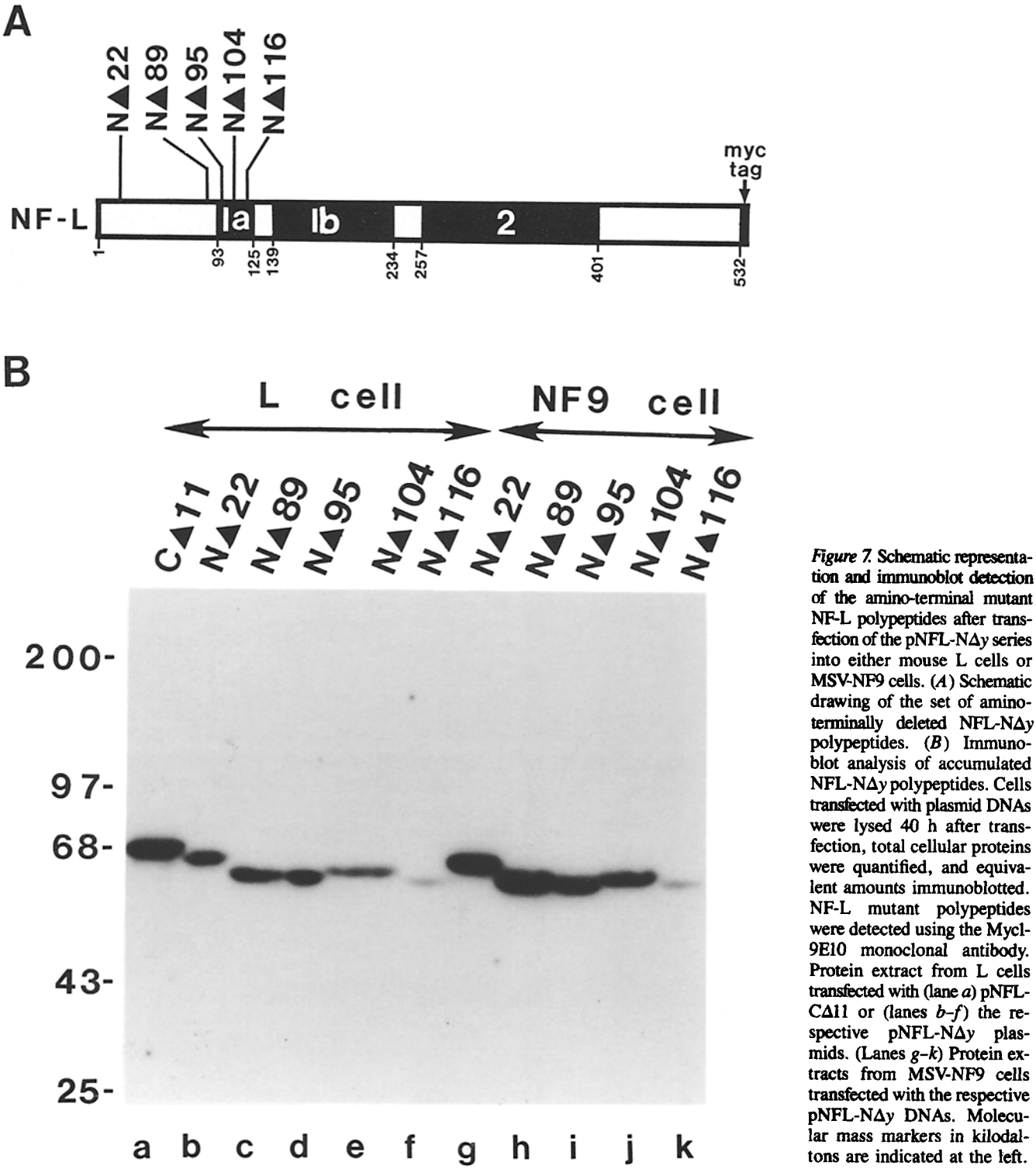

Figure 7. Schematic representation and immunoblot detection of the amino-terminal mutant NF-L polypeptides after transfection of the pNFL-NΔ*y* series into either mouse L cells or MSV-NF9 cells. (*A*) Schematic drawing of the set of amino-terminally deleted NFL-NΔ*y* polypeptides. (*B*) Immunoblot analysis of accumulated NFL-NΔ*y* polypeptides. Cells transfected with plasmid DNAs were lysed 40 h after transfection, total cellular proteins were quantified, and equivalent amounts immunoblotted. NF-L mutant polypeptides were detected using the Mycl-9E10 monoclonal antibody. Protein extract from L cells transfected with (lane *a*) pNFL-CΔ11 or (lanes *b–f*) the respective pNFL-NΔ*y* plasmids. (Lanes *g–k*) Protein extracts from MSV-NF9 cells transfected with the respective pNFL-NΔ*y* DNAs. Molecular mass markers in kilodaltons are indicated at the left.

Figure 8. Assembly properties of NF-L subunits missing portions or the entirety of the nonhelical amino-terminal domain. Mouse L cells grown on coverslips were transfected with plasmids (*A* and *B*) pNFL-NΔ22, (*C* and *D*) pNFL-NΔ18-31, (*E* and *F*) pNFL-NΔ89, and (*G* and *H*) pNFL-NΔ95. Cells were stained 40 h after transfection as described in Fig. 4 for (*A*, *E*, and *G*) NF-L subunits and for (*B*, *D*, *F*, and *H*) endogenous vimentin. Part *C* was stained for NF-L polypeptides using the monoclonal antibody to NF-L since this mutant NF-L is not tagged with the myc epitope. Bar, 10 μm.

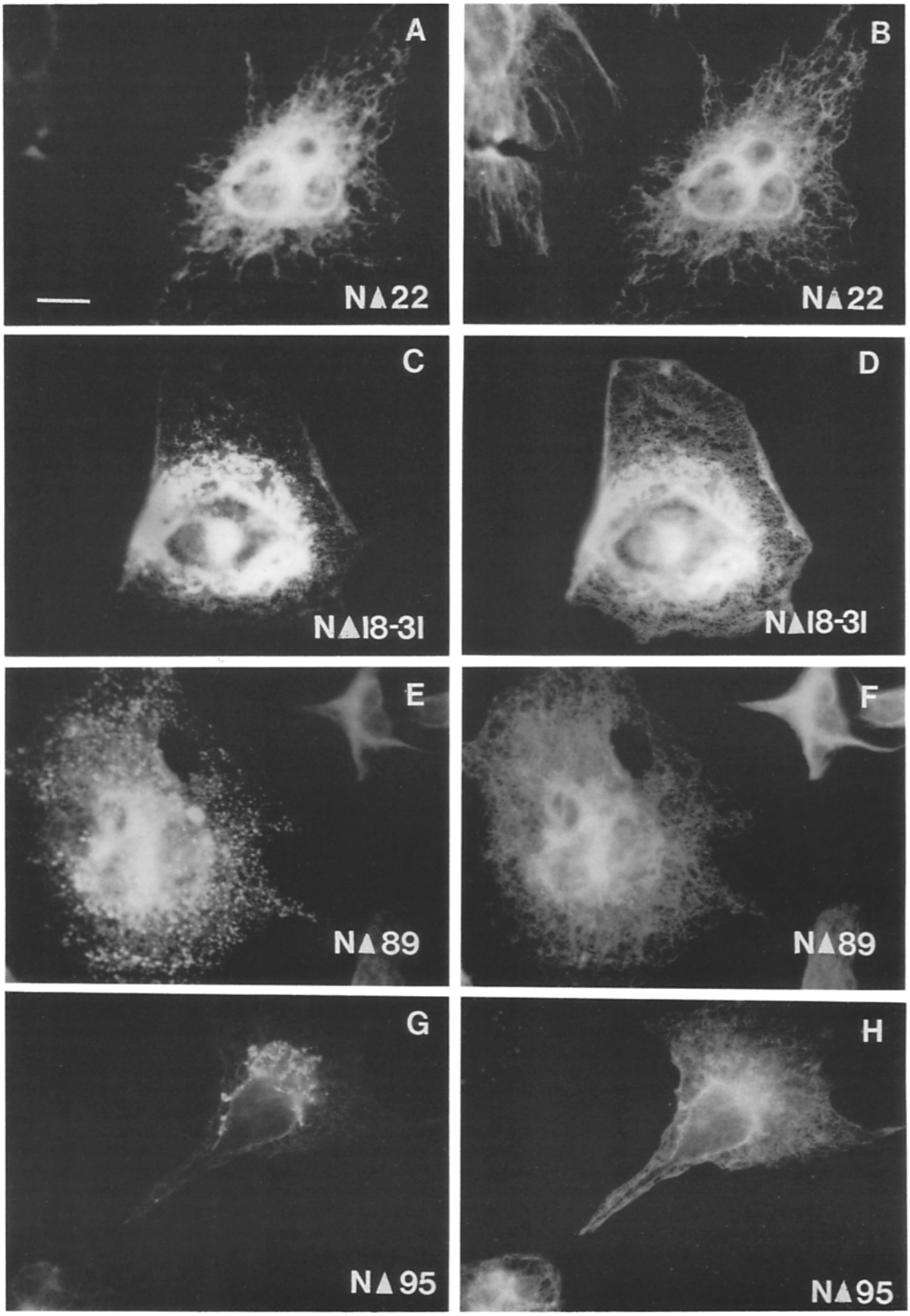
A
NΔ22
B
NΔ22
C
NΔ18-31
D
NΔ18-31
E
NΔ89
F
NΔ89
G
NΔ95
H
NΔ95

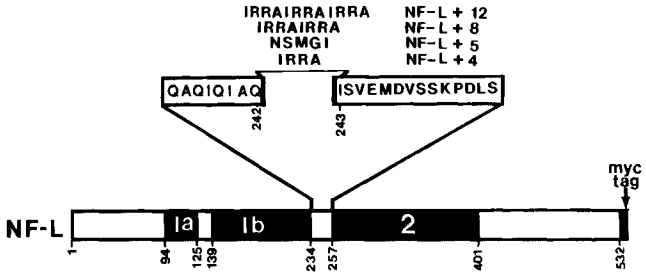

Figure 9. Schematic drawing of 4–12 amino acid insertions placed in the linker domain separating coils 1 and 2 of NF-L. Either a single 15-base segment or one, two or three 12-mer Bam HI linkers was inserted into the linker region (at the unique Bgl II site) between coils 1 and 2 of mouse NF-L. The schematic displays the predicted amino acid sequences in the linker region.

transiently transfected into L cells and the encoded NF-L subunits visualized by immunofluorescence. In most (80%) of the transfected cells, four and five amino acid insertions yielded subunits that were completely coaligned with the endogenous vimentin, which remained in an array indistinguishable from that in untransfected cells (Fig. 10, *A* and *B*). Even NF-L subunits containing an eight amino acid insertion (denoted NFL+8) localized with a wild-type vimentin array in ~ 50% of transfected cells (Fig. 10, *C* and *D*). Obviously, substantial flexibility does exist in this hinge domain. However, in the remaining 50% of cells expressing NFL+8, large perinuclear aggregates containing both the mutant NFL+8 and wild-type vimentin were accumulated (Fig. 10, *E* and *F*) in addition to some remaining filaments containing both NFL+8 and vimentin. Quantitative immunoblotting revealed the average ratio of NFL+8 to vimentin to be 1:10. We infer that accumulation below this level yielded coassembly and retention of a normal IF array, while at higher stoichiometries NFL+8 becomes network disrupting. Increasing the number of amino acids inserted to 12 yielded a nearly complete disruption of vimentin arrays in >90% of transfected cells (Fig. 10, *G* and *H*), although in cells presumably expressing lower amounts of NFL+12 some coassembly of the mutant with vimentin could be seen (not shown).

Discussion

The use of DNA transfection to force co-expression of NF-L subunits with either wild-type vimentin or NF-L polypeptides has uncovered domains essential for in vivo assembly of this neurofilament subunit. As in the case for NF-M (Wong and Cleveland, 1990), no mutation from either the amino or carboxy terminus that truncates into the predicted helical domain yields an assembly competent subunit. While this was the expected outcome, more surprising was the finding that the minimal NF-L domain that efficiently coassembled without disrupting normal IF arrays contained not only the expected rod domain, but also 75% of the head and nearly 50% of the tail. While it is true that at lower stoichiometries NF-L subunits retaining less of the tail do colocalize with wild-type arrays, all such subunits become assembly disruptors when present at higher levels.

The apparent necessity for substantial amounts of head and tail sequences stands in contrast to the situation reported for two other IF subunits, desmin and type I keratin. Both in vitro assembly studies using desmin from which only 29 amino acids of the tail remained after proteolysis (Kaufmann et al., 1985) or in vivo experiments using DNA transfection to express a desmin truncated in almost all of the tail (van den Heuval et al., 1987) found that such carboxy-terminally shortened desmin retained assembly competence. However, the differing requirement for the tail in assembly of desmin and NF-L may be more apparent than real. Since the amount of desmin accumulated in transfected cells was not measured, it is possible that such truncated subunits (like the case we have shown here for NF-L) are in fact assembly disruptors when accumulated in higher stoichiometries relative to wild-type subunits. Similarly interpretation of the in vitro experiments is complicated by the uncertainties of how in vitro conditions relate to in vivo properties. In fact, in vitro reassembly of truncated desmin (Kaufmann et al., 1985) indicated formation of apparently normal filaments under low salt conditions (50 mM) but abnormal, laterally aggregated products at more physiological salt (170 mM). This indicates that truncation of the tail does affect some aspect of filament organization, quite possibly in keeping neighboring filaments apart. For keratins, the only known IFs that are obligate heteropolymers of type I and type II chains, DNA transfection initially revealed that for one human type I keratin (K14) the entire tail domain was dispensible for coassembly in the presence of normal type I and II subunits (Albers and Fuchs, 1987). Here again the stoichiometry of the mutant and wild-type keratin subunits was not determined and a possible role of the tail in assembly or in establishing a filament array cannot be discounted, although the discovery of a wild-type bovine keratin that is nearly tailless (Bader et al., 1986) and that can be a prominent component in some epithelial cells suggests otherwise.

A more clear distinction between the assembly characteristics of NF and other IF subunits is in the properties of amino-terminal mutants. Transfection experiments have revealed that type I keratin retains competence for coassembly into IF arrays comprised of normal type I and type II keratins even when all but eight amino acids of the head are removed (Albers and Fuchs, 1989). Similarly, desmin truncated by in vitro proteolysis to remove two-thirds of its head domain retains full competence for coassembly with wild type up to ratios of 1:1, although the mutant fails to assemble on its own (Kaufmann et al., 1985). For NF-L (and NF-M; Wong and Cleveland, 1990), we find that little of the head can be removed without disrupting in vivo filament arrays even at much lower proportions of mutant to wild-type subunits. Indeed, truncation of the majority (or entirety) of the head do-

Figure 10. Expression in L cells of NF-L polypeptides containing insertions within the linker region between coils 1 and 2. L cells grown on coverslips were transfected with (*A* and *B*) pNFL+5, (*C–F*) pNFL+8, or (*G* and *H*) pNFL+12. Cells were stained 40 h after transfection as described in Fig. 4 for (*A*, *C*, *E*, and *G*) NF-L subunits and (*B*, *D*, *F*, and *H*) endogenous vimentin. Bar, 10 μm.

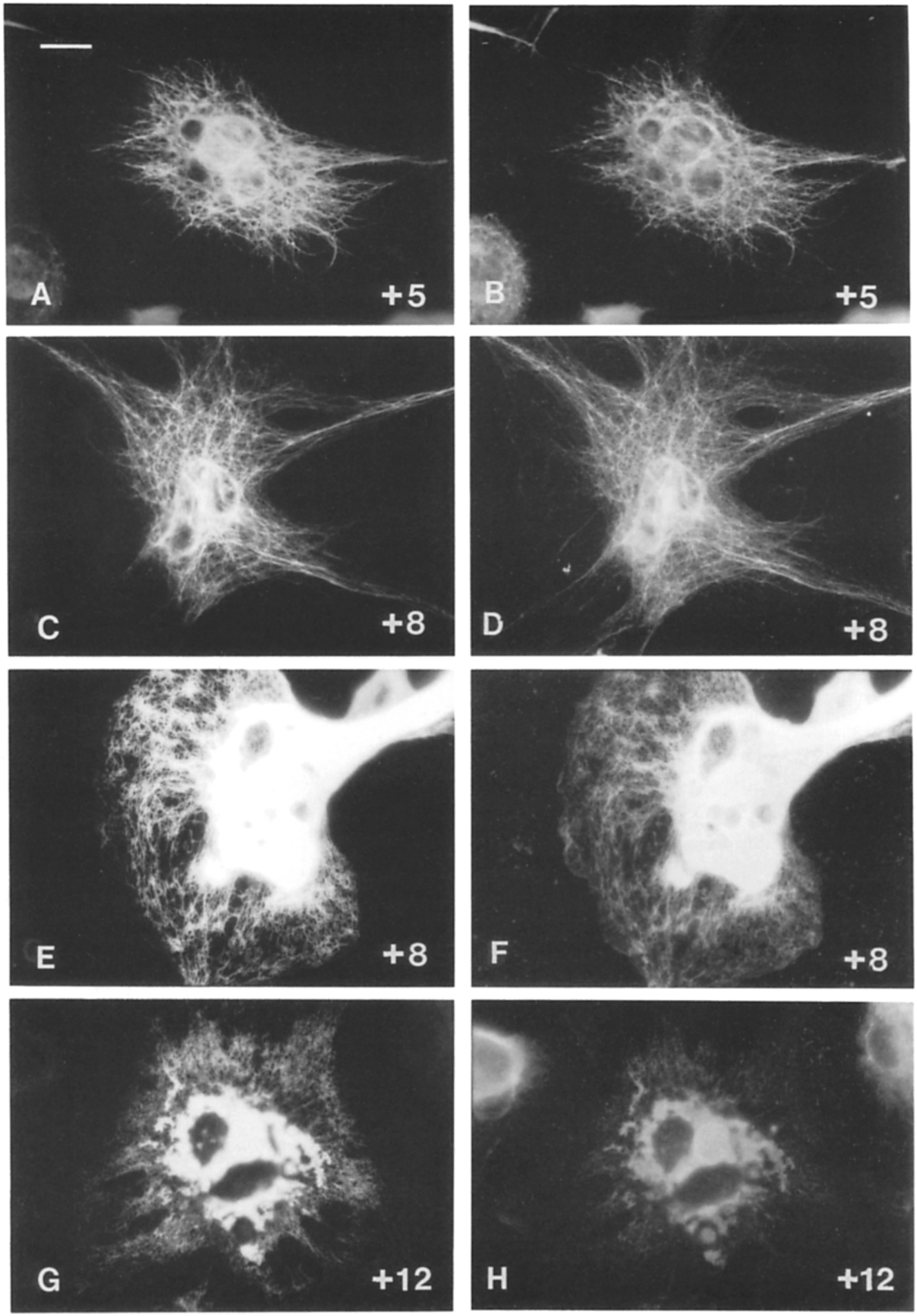
A
+5
B
+5
C
+8
D
+8
E
+8
F
+8
G
+12
H
+12

main of either NF-L or NF-M yields subunits that are pseudo-recessive and that neither assemble nor efficiently affect arrays assembled from coexpressed wild type IF subunits. In fact, the proteolytically truncated desmin (Kaufmann et al., 1985) also showed this recessive property: it assembled with desmin only if heterodimers/tetramers were first formed (by addition, then removal of a denaturant). The recessive amino-terminal mutants of NF-L differ from this desmin example (at least in vivo) since in the transfection experiments both mutant and wild type are synthesized together and still fail to coassemble. In any event, since NF-L bearing much smaller deletions in the head (e.g., only amino acids 18–31) are dominant disruptors of wild-type IF arrays, we infer that sequences between amino acids 31 and 78 of the head domain are necessary for an early step(s) in the assembly process. It is plausible to propose that the important sequences lie within the arginine-rich domain between 16 and 55, since such a basic domain is present in the heads of the nonepithelial IF subunits. That the head domain contains elements necessary for assembly of NF-L is reminiscent of an earlier effort with desmin that showed that in vitro phosphorylation of the head caused filament disassembly (Geisler and Weber, 1988) and the demonstration that phosphorylation of lamins at positions adjacent to both the amino- and carboxy-terminal borders of the helical domain (Heald and McKeon, 1990; Peter et al., 1990; Ward and Kirschner, 1990) causes cell cycle–dependent filament disassembly.

The most conserved feature of the IF proteins is the predicted helical domain spanning ~ 310 amino acids. This domain is distinguished both by the presence of a heptad repeat in which hydrophobic residues are found at positions 1 and 4 and by two short internal nonhelical segments that separate the helix into coils 1a and 1b, and 2. In most IF subunits (except for NF-M and NF-H), these linker regions contain helix-disrupting proline residues. Since the size of each linker is somewhat variable in length and sequence among the IF family, while the helical regions are nearly invariant in length (with the exception of the lamins), it has seemed plausible to think of these domains as hinges between the structurally conserved coils. In this context, we have now demonstrated that the hinge domain between coils 1b and 2 of NF-L can tolerate substantial mutation without affecting assembly competence. Insertion of four or five additional amino acids did not yield any observable phenotype, and even an eight amino acid addition retained competence for coassembly at lower stoichiometries. Obvious future experiments will be to test whether such flexibility is present at the linker domain between coils 1a and 1b.

Although the essentialness of the terminal portion of the rod domain may have seemed obvious since it contains the only truly conserved sequence domain (LLEGE) common to all IF subunits, our finding that expression of NF-L subunits truncated only a few residues into the rod domain uniformly yields disruption of the endogenous IF (vimentin or NF-L) array even when present in low amounts provides direct experimental support for a requirement of the rod domain. In conjunction with the earlier finding with a type I keratin (and our findings with NF-M; Wong and Cleveland, 1990), it seems safe to conclude that an intact rod domain is essential for productive filament assembly. At what step assembly is blocked and the actual structure(s) of the aggregated products remain to be examined (using electron microscopy of transfected cells and in vitro assembly assays). Without such additional efforts we cannot completely exclude the formal possibility that some of the assembly-disruptive properties of mutant subunits may result from the carboxy-terminal myc tag, although the apparent wild-type assembly of smaller deletion mutations makes this seem unlikely (see also the discussion in Wong and Cleveland [1990] concerning this and other important limitations to interpretation of cell transfection experiments).

But independent of this, the identification of potent, dominant mutants suggests a way to test experimentally the in vivo function of NF, a question that in fact remains unsettled for all IF subunits. For NF, a series of correlative studies have suggested that NF might be an intrinsic determinant of axonal diameter. Evidence for this arose initially from noting that NF content is closely correlated with cross-sectional area in the axons of large myelinated nerve fibers (Friede and Samorajski, 1970; Weiss and Mayr, 1971; Berthold, 1978). Moreover, reductions in NF expression are associated with decreased axonal caliber (Hoffman et al., 1985, 1987) after axonal injury. Also, radial growth of myelinated nerve fibers, which occurs during postnatal development, coincides temporally with the induction of NF gene expression (Muma, N., and P. Hoffman, unpublished data). We have completed the first phase of a test of this potential function by constructing transgenic mice harboring NF-L transgenes that express high levels of NF-L (four- to fivefold more than in wild-type mice) in peripheral axons. This study revealed clearly that the accumulation of additional filaments constructed primarily of NF-L did not affect axonal caliber, although the filaments in the resultant axons were partially disorganized (Monteiro et al., 1990). A more definitive test of the role NFs provide should now be possible by constructing additional mice that express one of the dominant, assembly-disrupting NF-L mutants identified here.

We thank Ms. Andrea Mook for her contributions to the construction of the linker insertions into NF-L and Mr. Mike Delanoy for help with the confocal microscopy. We also thank Drs. G. Shaw (University of Florida, Gainesville, FL) and Frank McKeon (Harvard Medical School, Boston, MA) for donating NF-L and lamin antibodies, respectively. Preliminary phases of this work were supported by a grant from the March of Dimes to D. W. Cleveland. Later phases were supported by National Institutes of Health (NIH) grant NS 27036 to D. W. Cleveland. S. R. Gill, P. C. Wong, and M. J. Monteiro were supported, in part, by postdoctoral fellowships from the NIH, the Muscular Dystrophy Association, and the Maryland Affiliate of the American Heart Association, respectively.

Received for publication 13 June 1990 and in revised form 19 July 1990.

Note Added in Proof. X. Lu and E. B. Lane (1990. *Cell.* 62:681–696) have recently reported coexpression of both wild-type and mutant type I and II keratin genes in fibroblast cells that accumulate no endogenous keratin filaments. Similar to our finding that a portion of the head and tail domains are required for assembly of NF-L, they found that keratin filament assembly requires intact amino- and carboxy-terminal domains on at least one of the two subunits.

References

Albers, K., and E. Fuchs. 1987. The expression of mutant epidermal keratin cDNAs transfected in simple epithelial and squamous cell carcinoma lines. *J. Cell Biol.* 105:791–806.

Albers, K., and E. Fuchs. 1989. Expression of mutant keratin cDNAs in epithelial cells reveals possible mechanisms for initiation and assembly of intermediate filaments. *J. Cell Biol.* 108:1477–1493.

Bader, B. L., T. M. Magin, M. Hatzfeld, and W. W. Franke. 1986. Amino

acid sequence and gene organization of cytokeratin no. 19, an exceptional tail-less intermediate filament protein. *EMBO (Eur. Mol. Biol. Organ.) J.* 5:1865–1875.

Berthold, C. H., 1978. Morphology of normal pheripheral axons. *In* Physiology and Pathobiology of Axons. S. G. Waxman, editor. Raven Press, New York. 3–63.

Bignami, A., T. Rajn, and D. Dahl. 1982. Localization of vimentin, the nonspecific intermediate filament protein, in embryonal glia in early differentiating neurons. *Dev. Biol.* 91:281–295.

Evans, G. I., G. K. Lewis, G. Ramsay, and J. M. Bishop. 1985. Isolation of monoclonal antibodies specific for human c-myc proto-oncogene product. *Mol. Cell. Biol.* 5:3610–3616.

Fisher, D. Z., N. Chaudhary, and G. Blobel. 1986. cDNA sequencing of nuclear lamins A and C reveals primary and secondary structural homology to intermediate filament proteins. *Proc. Natl. Acad. Sci. USA.* 83:6450–6454.

Fliegner, K. H., G. Y. Ching, and R. H. K. Liem. 1990. The predicted amino acid sequence of α-internexin is that of a novel neuronal intermediate filament protein. *EMBO (Eur. Mol. Biol. Organ.) J.* 9:749–755.

Franke, W. W. 1987. Nuclear lamins and cytoskeletal intermediate filament proteins: a growing multigene family. *Cell.* 48:38-4.

Friede, R. L., and T. Samorajski. 1970. Axon caliber related to neurofilaments and microtubules in sciatic nerve fibers of rats and mice. *Anat. Rec.* 167:379–388.

Gawlitta, W., M. Osborn, and K. Weber. 1981. Coiling of intermediate filaments induced by the microinjection of a vimentin-specific antibody does not interfere with locomotion and mitosis. *Eur. J. Cell Biol.* 26:83–90.

Geisler, N., and K. Weber. 1981. Self-assembly in vitro of the 68,000 molecular weight component of the mammalian neurofilament triplet proteins into intermediate-size filaments. *J. Mol. Biol.* 151:565–571.

Geisler, N., and K. Weber. 1982. The amino acid sequence of chicken muscle desmin provides a common structural model for intermediate filament proteins. *EMBO (Eur. Mol. Biol. Organ.) J.* 1:1649–1656.

Geisler, N., and K. Weber. 1986. Structural aspects of intermediate filaments. *In* Cell and Molecular Biology of the Cytoskeleton. J. W. Shay, editor. Plenum Publishing Corp., New York. 41–68.

Geisler, N., and K. Weber. 1988. Phosphorylation of desmin in vitro inhibits formation of intermediate filaments: identification of three kinase A sites in the amino-terminal head domain. *EMBO (Eur. Mol. Biol. Organ.) J.* 7:15–20.

Geisler, N., S. Kaufmann, S. Fischer, U. Plessmann, and K. Weber. 1983. Neurofilament architecture combines structural principles of intermediate filaments with carboxy-terminal extensions increasing in size between triplet proteins. *EMBO (Eur. Mol. Biol. Organ.) J.* 2:1295–1302.

Geisler, N., U. Plessmann, and K. Weber. 1985. The complete amino acid sequence of the major mammalian neurofilament protein (NF-L). *FEBS (Fed. Eur. Biochem. Soc.) Lett.* 182:475–478.

Heald, R., and F. McKeon. 1990. Mutations of phosphorylation sites in lamin A that prevent nuclear lamina disassembly in mitosis. *Cell.* 61:579–589.

Herdberg, K. L., and L. B. Chen. 1986. Absence of intermediate filaments in a human adrenal cortex carcinoma derived cell line. *Exp. Cell Res.* 163:509–517.

Hirokawa, N., M. A. Glicksman, and M. B. Willard. 1984. Organization of mammalian neurofilament polypeptides within the neuronal cytoskeleton. *J. Cell Biol.* 98:1523–1536.

Hisanaga, S., and N. Hirokawa. 1990. Molecular architecture of the neurofilament II. Reassembly process of neurofilament L protein in vitro. *J. Mol. Biol.* 211:871–882.

Hoffmann, P. N., and D. W. Cleveland. 1988. Neurofilament and tubulin expression recapitulates the developmental program during axonal regeneration: induction of a specific β-tubulin isotype. *Proc. Natl. Acad. Sci. USA.* 85:4530–4533.

Hoffman, P. N., J. W. Griffin, and D. L. Price. 1984. Control of axonal caliber by neurofilament transport. *J. Cell Biol.* 99:705–714.

Hoffman, P. N., G. W. Thompson, J. W. Griffin, and D. L. Price. 1985. Changes in neurofilament transport coincide temporally with alterations in the caliber of axons in regenerating motor fibers. *J. Cell Biol.* 101:1332–1340.

Hoffman, P. N., D. W. Cleveland, J. W. Griffin, P. W. Landes, N. J. Cowan, and D. L. Price. 1987. Neurofilament gene expression: a major determinant of axonal caliber. *Proc. Natl. Acad. Sci. USA.* 84:3472–3476.

Holtz, D., R. A. Tanaka, J. Hartwig, and F. McKeon. 1989. The CaaX motif of lamin A functions in conjunction with the nuclear localization signal to target assembly to the nuclear envelope. *Cell.* 59:969–977.

Julien, J.-P., F. Cote, L. Beaudet, M. Sidky, D. Flavell, F. Grosveld, and W. Mushynski. 1987*b*. Sequence and structure of the mouse gene coding for the largest neurofilament subunit. *Gene (Amst.).* 68:307–314.

Kaufman, E. K., K. Weber, and N. Geisler. 1985. Intermediate filament forming ability of desmin derivatives lacking either the amino-terminal 67 or the carboxy-terminal 27 residues. *J. Mol. Biol.* 185:733–742.

Klymkowsky, M. W. 1981. Intermediate filaments in 3T3 cells collapse after the intracellular injection of a monoclonal anti-intermediate filament antibody. *Nature (Lond.).* 291:249–251.

Laemmli, U. K. 1970. Cleavage of structural proteins during the assembly of the head of bacteriophage T4. *Nature (Lond.).* 227:680–685.

Lees, J. F., P. S. Shneidman, S. F. Skuntz, M. J. Carden, and R. A. Lazarini. 1988. The structure and organization of the human heavy neurofilament subunit NF-H. *EMBO (Eur. Mol. Biol. Organ.) J.* 7:1947–1958.

Lendahl, U., L. B. Zimmerman, and R. D. G. McKay. 1990. CNS stem cells express a new class of intermediate filament protein. *Cell.* 60:585–595.

Leonard, D. G. B., J. D. Gorham, P. Cole, L. A. Greene, and E. B. Ziff. 1988. A nerve growth factor-regulated messenger RNA encodes a new intermediate filament protein. *J. Cell Biol.* 106:181–193.

Levy, E., R. H. K. Liem, P. D'Eustacio, and N. J. Cowan. 1987. Structure and evolutionary origin of the gene encoding mouse NF-M, the middle molecular mass neurofilament protein. *Eur. J. Biochem.* 166:71–77.

Lewis, S. A., and N. J. Cowan. 1985. Genetics, evolution, and expression of the 68,000 mol. wt. neurofilament protein: isolation of a cloned cDNA probe. *J. Cell Biol.* 100:843–850.

Lewis, S. A., and N. J. Cowan. 1986. Anomolous placement of introns in a member of the intermediate filament multigene family: an evolutionary conundrum. *Mol. Cell. Biol.* 6:1529–1534.

Liem, R. K. H., and S. B. Hutchinson. 1982. Purification of individual components of the neurofilament triplet: filament assembly from the 70,000 dalton subunit. *Biochemistry.* 21:3221–3226.

Lin, J. J. C., and J. R. Feramisco. 1981. Disruption of the in vivo distribution of intermediate filaments in fibroblast through the microinjection of a specific monoclonal antibody. *Cell.* 24:185–193.

Lopata, M. A., and D. W. Cleveland. 1987. In vivo microtubules are copolymers of available β-tubulin isotypes: localization of each of six vertebrate β-tubulin isotypes using polyclonal antibodies elicited by synthetic peptide antigens. *J. Cell Biol.* 105:1707–1720.

Lopata, M. A., D. W. Cleveland, and B. Sollner-Webb. 1984. High level transient expression of a chloramphenicol acetyl transferase gene by DEAE-dextran mediated DNA transfection coupled with a dimethylsulfoxide or glycerol shock treatment. *Nucleic Acids Res.* 12:5707–5717.

McKeon, F. M., M. W. Kirschner, and D. Caputo. 1986. Homologies in both primary and secondary structure between nuclear envelope and intermediate filament proteins. *Nature (Lond.).* 319:463–468.

Monteiro, M. J., and D. W. Cleveland. 1989. Expression of NF-L and NF-M in fibroblasts reveals coassembly of neurofilament and vimentin subunits. *J. Cell Biol.* 108:579–593.

Monteiro, M. J., P. N. Hoffman, J. D. Gearhart, and D. W. Cleveland. 1990. Expression of NF-L in both neuronal and nonneuronal cells of transgenic mice: increased neurofilament density in axons without affecting caliber. *J. Cell Biol.* 111:1543–1557.

Munro, S., and H. R. B. Pelham. 1987. A C-terminal signal prevents secretion of luminal ER proteins. *Cell.* 48:899–907.

Myers, M. W., R. A. Lazzarini, V. M. Y. Lee, W. W. Schlaepfer, and D. L. Nelson. 1987. The human mid size neurofilament subunit: a repeated protein sequence and the relationship of its gene to the intermediate filament gene family. *EMBO (Eur. Mol. Biol. Organ.) J.* 6:1617–1626.

Napolitano, E. W., S. S. M. Chin, D. R. Colman, and R. H. K. Liem. 1987. Complete amino acid sequence and in vitro expression of rat NF-M, the middle molecular weight neurofilament protein. *J. Neurosci.* 7:2590–2599.

Parysek, L. M., and R. D. Goldman. 1988. Distribution of a novel 57 kDa intermediate filament (IF) protein in the nervous system. *J. Neurosci.* 8:555–563.

Peter, M., J. Nakagawa, M. Doree, J. C. Labbe, and E. A. Nigg. 1990. In vitro disassembly of the nuclear lamina and M-phase specific phosphorylation of lamins by cdc2 kinase. *Cell.* 61:591–602.

Portier, M.-M., P. Brachet, B. Croizat, and F. Gros. 1984. Peripherin, a new member of the intermediate protein family. *Dev. Neurosci.* 6:335–344.

Smith, P. K., P. I. Krohn, G. T. Hermanson, A. K. Mallia, F. H. Gartner, M. D. Provenzaus, E. K. Fujimoto, N. M. Goeke, B. J. Olson, and D. C. Klenk. 1985. Measurement of protein using bicinchonic acid. *Anal. Biochem.* 150:76–85.

Steinert, P. M., and D. R. Roop. 1988. Molecular and cellular biology of intermediate filaments. *Annu. Rev. Biochem.* 57:593–625.

Tokutake, S., R. H. K. Liem, and M. L. Shelanski. 1984. Each component of neurofilament assembles itself to make component-specific filament. *Biomed. Res.* 5:235–238.

van den Heuvel, R. M. M., G. J. J. M. van Eyes, F. C. S. Ramaekers, W. J. Quax, W. T. M. Vree Egberts, G. Schaart, T. M. Cuypers, and H. Bloemendal. 1987. Intermediate filament formation after transfection with modified hamster vimentin genes. *J. Cell Sci.* 88:475–482.

Venetianer, A., D. L. Schiller, T. Magin, and W. W. Franke. 1983. Cessation of cytokeratin expression in a rat hepatoma cell line lacking differentiated functions. *Nature (Lond.).* 305:730–733.

Weiss, P. A., and R. Mayr. 1971. Organelles of neuroplasmic ("axonal") flow: neurofilaments. *Proc. Natl. Acad. Sci. USA.* 68:846–850.

Wong, P. C., and D. W. Cleveland. 1990. Characterization of dominant and recessive assembly defective mutations in mouse neurofilament NF-M. *J. Cell Biol.* 111:1987–2003.